Effects of Noncovalent and Covalent FAD Binding on the Redox and Catalytic Properties of *p*-Cresol Methylhydroxylase†

Igor Efimov, Ciarán N. Cronin, and William S. McIntire*

Molecular Biology Division, Department of Veterans Affairs Medical Center, San Francisco, California 94121, and Department of Biochemistry and Biophysics, University of California, San Francisco, California 94143

Received July 14, 2000; Revised Manuscript Received November 15, 2000

ABSTRACT: Each flavoprotein subunit (α or PchF) of the $\alpha_2\beta_2$ flavocytochrome *p*-cresol methylhydroxylase (PCMH) from *Pseudomonas putida* contains FAD covalently attached to Tyr384. PCMH oxidizes *p*-cresol to 4-hydroxybenzyl alcohol, which is oxidized subsequently by PCMH to 4-hydroxybenzaldehyde. The Y384F mutant form of PchF (apo-PchF[Y384F]) displayed stoichiometric noncovalent FAD binding. PchF-[Y384F]FAD associated with the cytochrome subunit (*β* or PchC) (producing PCMH[Y384F]), although not as avidly as with wild-type PchF containing covalently bound FAD ($PchF^C$). Dramatic increases in the two-electron $E_{m,7}$ (NHE) values for FAD were observed when it bound noncovalently to either apo-PchF or apo-PchF[Y384F], and the two-electron $E_{m,7}$ value for FAD was increased further by about 75 mV upon covalent binding to PchF, i.e., $PchF^C$. The $E_{m,7}$ values increased by approximately 20 and 45 mV, respectively, when $PchF^C$ and PchF[Y384F]FAD associated with PchC. The two-electron $E_{m,7}$ for covalently bound FAD in PCMH is 84 mV, the highest measured for a flavoprotein. The values for the one-electron redox potentials ($E_{m,7}$, NHE) for FAD were measured also for various forms of PchF. Under anaerobiosis, the reduction of PchF[Y384F]FAD by substrates was similar to that observed previously for PchF containing noncovalently bound FAD. Stopped-flow kinetic studies indicated a rapid substrate reduction of the FAD and heme in PCMH[Y384F] which produced $PchF[Y384F]FAD_{rad}$·PchC, the mutant enzyme containing the flavin radical and reduced heme. These experiments also revealed a slow reduction of unassociated $PchC_{ox}$ by $PchF[Y384F]FAD_{rad}$·PchC. Steady-state kinetic studies of the reaction of PCMH-[Y384F] with *p*-cresol indicated that the K_m for this substrate was unchanged relative to that of PCMH, but that the k_{cat} was diminished by an order of magnitude. The data indicate that the covalent attachment of FAD to PchF assists catalysis by raising the $E_{m,7}$ of the flavin. Contributions to this effect likely result from conformational changes.

The $\alpha_2\beta_2$ flavocytochrome *p*-cresol methylhydroxylase (PCMH,[1] EC 1.17.99.1) from *Pseudomonas putida* NCIMB 9869 contains FAD covalently attached at its 8α-carbon to the phenolate oxygen of Tyr384 in each α subunit. The stable, unassociated α_2 flavoprotein ($PchF_2$) and the unassociated *β* cytochrome subunit (PchC) may be obtained by isoelectric focusing of PCMH (*1*). Recently, we reported the construction of expression vectors for the production of PchF in *Escherichia coli* (*2*) and for the production of PchC in *Pseudomonas aeruginosa* (*3*). FAD binds noncovalently and tightly to the recombinant apo-PchF. A detailed comparison of the properties of PchF containing both covalently bound ($PchF^C$) and noncovalently bound FAD ($PchF^{NC}$) has been reported (*2*).

There were significant differences in the redox properties for $PchF^C$ and $PchF^{NC}$. For example, *p*-cresol was virtually incapable of anaerobically reducing $PchF^{NC}$, whereas stoichiometric 4-hydroxybenzyl alcohol reduction of $PchF^{NC}$ was relatively rapid. Surprisingly, during an anaerobic *p*-cresol titration of $PchF^C$, 2 electron equiv/mol of substrate was consumed. This contrasts with an anaerobic PCMH titration, which consumed 4 electron equiv/mol of *p*-cresol, 2 from *p*-cresol and 2 from its oxidation product 4-hydroxybenzyl alcohol (*4*). The lower stoichiometry for $PchF^C$ was attributed to a slow release of 4-hydroxybenzyl alcohol from the reduced form of this protein. In the absence of *p*-cresol, the alcohol rapidly and stoichiometrically reduced $PchF^C$ (*2*). The difference in the redox properties of $PchF^C$ and $PchF^{NC}$ could be attributed to structural dissimilarities at the active site, to differences in the redox potentials of the bound FAD, or to both. A reliable and reproducible procedure (*5*) has now been used to determine the values of the two-electron redox potentials ($E_{m,7}$, NHE) for the FAD bound to $PchF^C$ and to PCMH. This method has also been used to determine

† This research was supported by a Department of Veterans Affairs Merit Review Grant and a Program Project Grant (HL-16251) from the National Heart, Lung and Blood Institute of the National Institutes of Health.

* To whom correspondence should be addressed: Molecular Biology Division (151-S), Department of Veterans Affairs Medical Center, 4150 Clement St., San Francisco, CA 94121. Telephone: (415) 387-1431. Fax: (415) 750-6959. E-mail: wsm@itsa.ucsf.edu.

[1] Abbreviations: DCIP, 2,6-dichlorophenolindophenol; ox, rad, and red (subscripts), oxidized, radical, and reduced, respectively; PchF (α) and PchC (*β*), flavoprotein and cytochrome subunits of *p*-cresol methylhydroxylase, respectively; $PchF^C$ and $PchF^{NC}$, wild-type PchF with covalently bound and noncovalently bound FAD, respectively; PchF[Y384F]FAD and PchF[Y384F], Y384F mutant of PchF with and without noncovalently bound FAD, respectively; PCMH[Y384F], $\alpha_2\beta_2$ flavocytochrome complex between PchF[Y384F]FAD and PchC; PCMH, $\alpha_2\beta_2$ *p*-cresol methylhydroxylase; PES, phenazine ethosulfate; VAO, vanillyl alcohol oxidase.

10.1021/bi001644m CCC: $20.00
Published on Web 01/30/2001

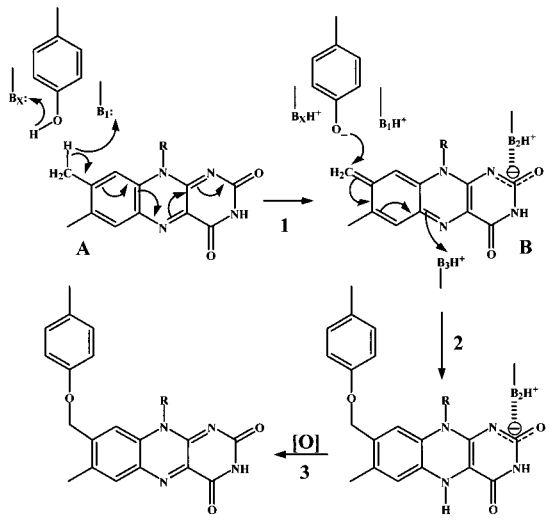

FIGURE 1: Proposed mechanism for the covalent flavinylation of Tyr384 in PchF. The flavinylation process occurs only following the binding of PchC to PchF^{NC} (*2*, *9*). B_X, B_1, B_2, and B_3 are bases in PchF^{NC} that are in proximity to the FAD. Base B_X removes the phenolic proton from Tyr384, while base B_1 removes a proton from the 8α-carbon of the isoalloxazine ring of FAD, which results in the formation of the essential iminoquinone methide intermediate. An increase in the two-electron $E_{m,7}$ of the flavin would make the 8α-proton more acidic, thus facilitating the covalent flavinylation process. An increase in the $E_{m,7}$ would also make the iminoquinone methide more electrophilic.

the two-electron $E_{m,7}$ values for the FAD bound to PchF^{NC}, for a site-specific mutant form of PchF in which Tyr384 has been replaced with a phenylalanyl residue (PchF[Y384F]-FAD) and for PCMH[Y384F]. A variation of this procedure allowed us to estimate the one-electron potentials for (A) the conversion of oxidized FAD to the flavin semiquinone anionic ("red") radical and (B) the conversion of the red radical to the fully two-electron reduced FAD for each protein species.

As described herein, the values of the two-electron $E_{m,7}$ of the FAD in all of the above-mentioned proteins are different, and if it is assumed that there are minimal structural changes at the flavin−substrate binding region, then it can be concluded that the covalent tethering of FAD to the polypeptide alters the $E_{m,7}$ in a manner more conducive to catalysis. This conclusion was offered by others studying vanillyl alcohol oxidase (VAO) from *Penicillium simplicissimum*, an enzyme similar to PCMH in structure (*6*) and in the reaction it catalyzes (*7*). For VAO, the FAD is covalently attached to His422. The X-ray structure of VAO[H422A] (*7*) indicated that minimal structural changes had occurred at the substrate−FAD binding sites when compared to the wild-type VAO structure (*8*). However, as proffered herein, conformational changes at the FAD binding site of PchF likely contribute also to alterations of its redox properties.

Previously (*2*, *9*), we reported that covalent tethering of FAD occurred only when PchF^{NC} was exposed to PchC. Since PchC is unable to associate with apo-PchF, FAD binding must effect structural changes that allow PchF^{NC} to conjoin with PchC. This association produces additional structural changes in PchF^{NC} that promote covalent FAD linkage to Tyr384 and result in avid PchC binding (*1*, *10*). The covalent binding results in two-electron-reduced FAD (Figure 1). These electrons are shuttled from the fully reduced FAD to an external electron acceptor via PchC, the same route employed by PCMH during turnover following reduction by substrate.

To understand better the mechanism of covalent flavinylation, it is desirable to study the properties of all of the intermediates in this process. Unfortunately, the PchF^{NC}−PchC intermediate does not accumulate when PchC and PchF^{NC} are mixed. Since FAD cannot covalently bind to PchF[Y384F], this form of PchF provides a means of studying this complex. This report presents the UV−visible spectral, biochemical, and redox properties of PchF[Y384F]-FAD and PCMH[Y384F] and compares these to the properties of PchF^{C}, PchF^{NC}, and PCMH (*2*).

MATERIALS AND METHODS

Materials. Sodium dithionite (Kodak Chemical Co.), disodium 2,6-dichlorophenol indophenol (DCIP) (General Biochemicals, Inc.), glucose oxidase (Miles Laboratories), thionin (Janssen Chimica), toluylene blue (ICN Pharmaceuticals, Inc.), and other reagents (Sigma Chemical Co. or Aldrich Chemical Co.) were from the indicated sources. 4-Hydroxybenzyl alcohol, 4-hydroxybenzaldehyde, and 4-bromophenol were purified as reported previously (*2*). Oligonucleotides were from Operon Technologies, Inc. Routine cloning manipulations utilized *E. coli* DH5αF′IQ (Life Technologies, Inc.) as the host.

Y384F Site-Directed Mutagenesis of PchF. The Phe replacement of Tyr384 in PchF was carried out according to the procedures of Deng and Nickoloff (*11*) by using the Clontech Transformer Site-Directed Mutagenesis Kit with the modification noted previously (*12*). The template, pUC-PchFf, for this procedure was pUC19 containing a 627 bp *Asp*718−*Bam*HI DNA fragment from the 3′-end of the *PchF* coding sequence (*13*), derived from plasmid pKS-PchF (*2*), and cloned into the same sites of pUC19. The mutagenesis was carried out by using Trans Oligo *Nde*I−*Nco*I (5′-pGAG TGC ACC ATG GGC GGT GTG AAA T-3′) as the selection primer (provided with the kit) and oY384F (5′-pGGA ATT CGG CCT GTT CAA CTG GCG TGG G-3′) as the mutagenic primer. The underlined bases differ from those of the target template. The DNA insert of a selected mutant clone (identified by elimination of the unique *Bsr*GI site) was entirely sequenced on both strands to confirm the integrity of the mutagenesis process. The internal *Asp*718−*Bsu*36I fragment of this clone was used to replace the native *Asp*718−*Bsu*36I fragment in the PchF expression vector pET-PchF (*2*) to produce pET-PchF[Y384F]. *E. coli* BL21-(DE3) transformed with pET-PchF[Y384F] was used for the production of the recombinant protein. DNA sequence determinations and computer analysis of DNA sequence data were carried out as described previously (*12*).

Purification of PchF[Y384F]. Bacterial growth and the apo-PchF[Y384F] purification were as described for apo-PchF (*2*). The protein was released from the *E. coli* periplasm by using Polymixin B. Q-Sepharose (Pharmacia Amersham Biotech) and Macro-Prep Ceramic Hydroxyapatite (type I, 20 μm) (Bio-Rad Laboratories) chromatographies removed *E. coli* cytochromes and FAD, respectively, and other contaminating components (*2*). Last, chromatofocusing was carried out on a Mono P HR 5/20 column (Pharmacia Amersham Biotech). After equilibration with 25 mM 1,3-bis[tris(hydroxymethyl)methylamino]propane-HCl buffer (pH

6.4), the protein was applied at a flow rate of 1 mL/min. After the column had been washed with this buffer for 1 min, a pH gradient was initiated by switching to a 6% (v/v) solution of Polybuffer 74 (Pharmacia Amersham Biotech), adjusted to pH 3.95 with HCl. Apo-PchF[Y384F] eluted at ~19 min (pH ~5.0). Immediately after elution, the pH of the apo-PchF[Y384F] sample was adjusted to ~7 by adding 1 M KH_2PO_4-KOH buffer (pH 7.2). The Polybuffer components were removed by several rounds of centrifugation and concentration (Centricon-30 concentrator, Amicon, Inc.), using 100 mM KH_2PO_4-KOH buffer (pH 7.2). The yield was 25−30 mg of pure apo-PchF[Y384F] from 25 g of cell paste.

Steady-State Kinetic Assays. Phenazine ethosulfate (PES)/DCIP as well as horse heart cytochrome *c* assays were carried out as described previously (*4*, *14*).

UV−Visible and Fluorescence Spectroscopy. The $E_{m,7}$ measurements were carried out in 25 mM KH_2PO_4-KOH buffer (pH 7.0) at 25 °C. Other experiments were carried out in 25 mM KH_2PO_4-KOH buffer (pH 7.4) at 25 °C. A Hewlett-Packard 8453 diode array spectrophotometer was used to obtain the UV−visible spectra. Anaerobic titrations and the $E_{m,7}$ measurements were carried out in anaerobic quartz cuvettes (*15*). Due to their volatility, *p*-cresol solutions were made anaerobic by using glucose, glucose oxidase, and catalase (*2*). Other solutions were made anaerobic by several cycles of vacuum and argon flushing. PchC was reduced by exposure to light in the anaerobic buffer containing 25 mM EDTA and 0.2 μM 5-deazariboflavin (*16*). The *p*-cresol and 4-hydroxybenzyl alcohol concentrations were determined by using an ϵ of 1.71 mM^{-1} cm^{-1} at 276 and 273 nm (*17*), respectively. Anaerobic dithionite solutions were standardized by titrating anaerobic solutions of FAD (ϵ_{445} = 11.3 mM^{-1} cm^{-1}). The concentrations of PchF[Y384F]FAD solutions were determined by using an ϵ_{440} of 12.6 mM^{-1} cm^{-1} (*2*). The concentrations of apo-PchF[Y384F] solutions were calculated by using an ϵ_{280} of 80.8 mM^{-1} cm^{-1} (*18*). The concentrations of $PchC_{ox}$ and $PchC_{red}$ solutions were calculated from the ϵ_{552}(red) − ϵ_{552}(ox) value of 19 mM^{-1} cm^{-1} (*4*). Each set of titration spectra was analyzed by Factor Analysis using the SPECFIT program (Spectrum Software Associates, Chapel Hill, NC) to extract dissociation constants and the spectrum of each independent component.

Protein two-electron potentials were determined with respect to the $E_{m,7}$ values of appropriate dyes, by using xanthine and xanthine oxidase (300 μM and 50−100 nM, respectively) as the source of electrons in the presence of 2 μM methyl viologen as the mediator (*5*). For each anaerobic (vide supra) mixture in an anaerobic cuvette, the reaction was initiated by the addition of xanthine oxidase from the sidearm of the cuvette. The course of the two-electron reduction of protein-bound FAD and the reference dye was followed by recording spectra at various times thereafter. At each time, the concentrations of oxidized and reduced dye and oxidized and reduced protein-bound FAD were determined by a Factor Analysis of the spectral data using the SPECFIT program. To determine the $E_{m,7}$ values for the two one-electron redox couples for $PchF^{C}$, $PchF^{NC}$, PchF-[Y384F]FAD, PCMH, and PCMH[Y384F], these proteins were reduced by the xanthine−xanthine oxidase method, in the presence of methyl viologen, but in the absence of the reference dye. The solutions contained 20 μM methyl viologen, 5−10 μM protein, 50 nM xanthine oxidase, and 300 μM xanthine in 25 mM KH_2PO_4-KOH buffer (pH 7.0) at 25 °C, and the complete two-electron reduction of the FAD in each protein proceeded with the intermediate formation of a high level of the anionic flavin radical.

Fluorescence quenching titrations were performed by using a Hitachi F-4010 fluorescence spectrofluorometer. The excitation and emission wavelengths were 280 and 340 nm for tryptophan and 446 and 520 nm for FAD, respectively. PchC (1 and 3 μM) was titrated with $PchF^{C}$ or PchF[Y384F]-FAD. The fluorescence quenching of the PchF tryptophyl residues was assessed. FAD fluorescence quenching provided a measure of its level of binding to apo-PchF[Y384F].

Stopped-Flow Kinetic Experiments. The OLIS RSM-1000 rapid spectrum scanning stopped-flow apparatus (On-Line Instrument Systems, Inc., Bogart, GA) was used in the wavelength range from 350 to 650 nm, at 25 or 6 °C in aerobic solutions. Spectra were recorded each millisecond for a total of 4000 ms. Spectra and kinetic constants were computed by using the OLIS Factor Analysis software.

Data Analysis. Data were fitted to the appropriate nonlinear equations by regression analyses using the NONLIN program (P. H. Sherrod, Nashville, TN). For data where dependent variables had standard errors, these errors were propagated by using their values as weights for linear or nonlinear regression analyses following a procedure published previously (*14*).

RESULTS

Properties of PchF[Y384F]. Pure apo-PchF[Y384F] was stable in frozen solution for several months at pH 7.5 and −20 °C. An FAD fluorescence quenching titration indicated that it bound rapidly and stoichiometrically to apo-PchF-[Y384F] (data not shown). To measure the affinity of PchF-[Y384F]FAD for PchC, the fluorescence quenching of PchF[Y384F]FAD tryptophyl residues by PchC was monitored. This approach was tested with $PchF^{C}$ and PchC, which bind stoichiometrically to each other, and with apo-PchF and pchC, which do not bind (*2*). The data (not shown) indicated that PchC bound tightly to $PchF^{C}$, whereas in the latter case, binding (quenching) was not observed. The data for PchF-[Y384F]FAD and PchC (not shown) indicated an association of the two proteins, although the affinity was lower than that of $PchF^{C}$ for PchC. The high concentrations of PchC (>2 μM) produced concentration-dependent internal fluorescence quenching, which precluded accurate estimates of K_D values.

It was found that the reduced form of PchC ($PchC_{red}$) bound more tightly than the oxidized form ($PchC_{ox}$) to PchF-[Y384F]FAD. $PchC_{ox}$ could be separated from a mixture of $PchC_{ox}$, PchF[Y384F]FAD, PCMH[Y384F], and PchF-[Y384F]FAD·$PchC_{red}$ by ceramic hydroxyapatite chromatography.[2] This treatment resulted in the isolation of apo-PchF[Y384F], free $PchC_{ox}$, and PchF[Y384F]FAD·$PchC_{red}$. Oxidation of PchF[Y384F]FAD·$PchC_{red}$ by potassium ferricyanide, and subsequent chromatography on a hydroxyapatite column, separated completely $PchC_{ox}$ from PchF-

[2] Wild-type and site-specifically altered PchF exist as dimers, i.e., $PchF_2$ and $(PchF[Y384F]FAD)_2$. However, each PchF subunit behaves as an independent enzyme molecule; i.e., there is no evidence for allosteric interactions between the associated PchF subunits. Thus, the wild-type flavoprotein and its Y384F mutant are termed and treated as monomers.

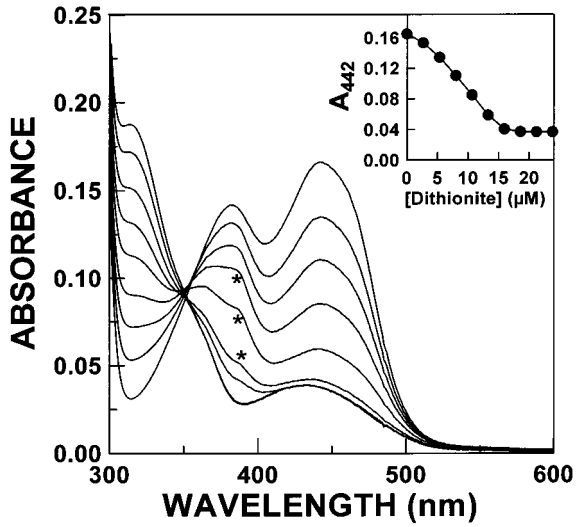

FIGURE 2: Anaerobic titration of PchF[Y384F]FAD with sodium dithionite. The titration of 12.6 μM PchF[Y384F]FAD (monomer concentration) was carried out in 25 mM KH_2PO_4-KOH buffer (pH 7.4) at 25 °C. The final concentrations of dithionite were 0, 2.67, 5.33, 7.99, 10.6, 13.3, 15.9, 18.6, 21.2, and 23.8 μM; the spectrum for 2.67 μM dithionite has been omitted for clarity. The asterisks denote spectra that suggest the presence of the anionic flavin radical; the radical has a λ_{max} at 385 nm (*2*). The inset shows a plot of the absorbance at 442 nm as a function of the total concentration of dithionite in the anaerobic protein solution.

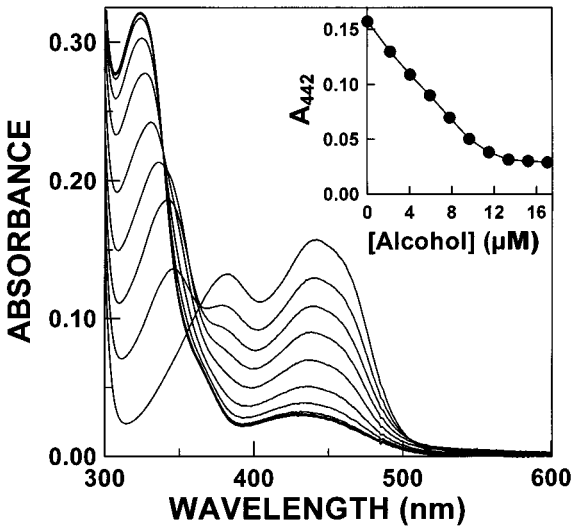

FIGURE 3: Anaerobic titration of PchF[Y384F]FAD with 4-hydroxybenzyl alcohol. The titration of 12.4 μM PchF[Y384F]FAD (monomer concentration) was carried out in 25 mM KH_2PO_4-KOH buffer (pH 7.4) at 25 °C. The final concentrations of alcohol were 0, 2.13, 4.02, 5.90, 7.77, 9.64, 11.5, 13.3, 15.2, and 17.0 μM. The inset shows a plot of the absorbance at 442 nm as a function of the total concentration of alcohol. The peak at 324 nm has absorbance contributions from the bound aldehyde and the reduced flavin (*2*).

[Y384F]. To increase the yield of PchF[Y384F]FAD·$PchC_{red}$, PchC was photochemically reduced anaerobically before mixing with PchF[Y384F]FAD.

PchF[Y384F]FAD·$PchC_{red}$ was capable of catalyzing the oxidation of *p*-cresol via a ping-pong type mechanism. For the PES/DCIP assay [25 mM KH_2PO_4-KOH buffer (pH 7.5) at 25 °C], $k_{cat} = 3.77 \pm 0.20$ s^{-1}, $K^{p\text{-cresol}} = 5.54 \pm 0.82$ μM, and $K^{PES} = 0.426 \pm 0.046$ mM. These values may be compared with those obtained for wild-type PCMH: $k_{cat} = 152 \pm 18$ s^{-1}, $K^{p\text{-cresol}} = 13.7 \pm 2.0$ μM, and $K^{PES} = 5.78 \pm 0.98$ mM (*9*). The following kinetic constants were determined when using horse heart cytochrome *c* as the electron acceptor [5 mM Tris-HCl buffer (pH 7.5) at 25 °C]: $k_{cat} = 7.0 \pm 0.3$ s^{-1}, $K^{p\text{-cresol}} = 2.20 \pm 0.23$ μM, and $K^{cyt} = 4.77 \pm 0.47$ mM. For PCMH, the comparable parameters are 98.5 ± 0.2 s^{-1}, 15.8 ± 0.8 μM, and 0.27 ± 0.01 mM, respectively (*14*).

Spectral Properties of PchF[Y384F]FAD. The PchF[Y384F]FAD UV−visible spectrum is identical to that of $PchF^{NC}$ (*2*), with absorbance maxima at 440 and 382 nm ($\epsilon_{440} = 12.6$ mM^{-1} cm^{-1} and $\epsilon_{384} = 10.0$ mM^{-1} cm^{-1}). A titration with the reductant sodium dithionite (Figure 2) produced spectra that were essentially the same as those observed during a $PchF^{NC}$ dithionite titration (*2*). The double-peak feature for intermediate spectra (the asterisks in Figure 2) and the lack of an isosbestic point in the 350 nm region suggest that a trace of the anionic flavin radical ($\lambda_{max} = 385$ nm) formed during the titration (*2*).

Titrations of $PchF^{NC}$, $PchF^{C}$ (*2*), and PchF[Y384F]FAD with *p*-cresol or nonreducing substrate analogues indicated that the electron-rich π system of the anionic forms of these phenolic compounds interacts with the electron-poor tricyclic π electron aromatic system of FAD, although unlike the anaerobic titration of $PchF^{NC}$ with *p*-cresol (*2*), a charge transfer band due to the interaction of *p*-cresol with FAD was not observed for PchF[Y384F]FAD, even after the addition of excess substrate. The time-dependent changes in the spectrum were consistent with an extremely slow reduction of the bound FAD (data not shown), but faster than that observed for the *p*-cresol reduction of $PchF^{NC}$ (*2*). The anaerobic reductive PchF[Y384F]FAD titration with 4-hydroxybenzyl alcohol (Figure 3) proceeded in the same manner as the analogous titration of $PchF^{NC}$ (*2*). Rapid reduction was accompanied by stoichiometric formation of 4-hydroxybenzaldehyde. Figure 4 displays the results of a titration of oxidized PchF[Y384F]FAD with nonreducing 4-hydroxybenzaldehyde. Factor Analysis of the data provided a K_D value of 0.47 ± 0.19 μM. As with $PchF^{NC}$ and $PchF^{C}$, the bathochromic shift observed for the maximal absorbance of bound aldehyde (343 nm) with respect to the free aldehyde (330 nm) indicates that the bound aldehyde adopts an anionic quinone methide-type tautomer (*2*). The absorbance in the 500−600 nm region is due to an aldehyde−FAD charge transfer complex (*2*). A titration of PchF[Y384F]FAD with the nonreducing substrate analogue 4-bromophenol produced significant changes in the spectrum, including the formation of a charge transfer peak with a λ_{max} of 620 nm (data not shown), as observed for the analogous titrations of $PchF^{NC}$ and $PchF^{C}$ (*2*).

Spectral Properties of PCMH[Y384F]. Figure 5 shows the equilibrium spectra resulting from the anaerobic *p*-cresol titration of an equimolar mixture of PchF[Y384F]FAD and $PchCC_{ox}$. Upon addition of substoichiometric amounts of substrate, PchC became fully reduced before two-electron reduction of the bound FAD was observed, indicating that intra- and intermolecular electron transfers must occur for PchC to remove both electrons from the substrate-reduced FAD. Factor Analysis provided three independent spectra (Figure 5): that of the oxidized protein, of PchF[Y384F]-FAD_{ox}·$PchC_{red}$, and of three-electron PCMH[Y384F]. As with PCMH (*4*), *p*-cresol delivers 4 electron equiv to the system (2 from *p*-cresol and 2 from its oxidation

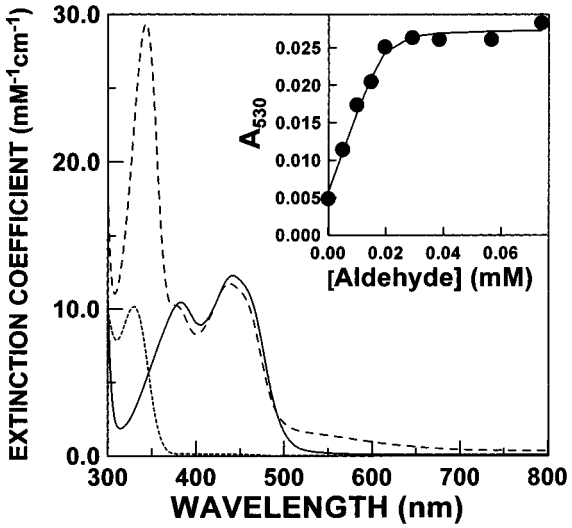

FIGURE 4: Aerobic titration of PchF[Y384]FAD with 4-hydroxybenzaldehyde. The titration was carried out in 25 mM KH_2PO_4-KOH buffer (pH 7.4) at 25 °C. The SPECFIT-generated spectra (see Materials and Methods) for the independent species involved in the titration of 12.4 mM PchF[Y384F]FAD with 4-hydroxybenzaldehyde are displayed. The spectra are for PchF[Y384F]FAD (—), the PchF[Y384F]FAD·aldehyde complex (— — —), and the unassociated aldehyde (- - -). The inset shows the change in absorbance at 530 nm due to aldehyde binding. A K_D of 0.47 μM was estimated from a global Factor Analysis using the SPECFIT program.

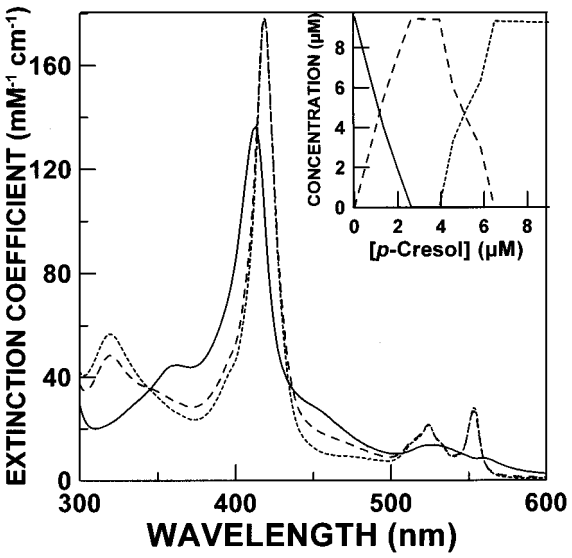

FIGURE 5: Anaerobic titration of PCMH[Y384F] with *p*-cresol. The titration of 9.5 μM PCMH[Y384F] (heterodimer concentration) was carried out in 25 mM KH_2PO_4-KOH buffer (pH 7.4) at 25 °C. The reduction proceeded in two stages. The first stage was a complete reduction of PchC (1 electron equiv/mol of PCMH[Y384F]). The second stage represents the two-electron reduction of the FAD. For approximately the first 60% of the PchC reduction, the reaction was rapid, whereas for the remainder of the titration, it required up to 20 min to reach the spectral end points. There was no indication of the formation of a flavin radical during this titration. The large frame displays the SPECFIT-generated spectra of all of the independent species: PCMH[Y384F] (—), the PchF[Y384F]-FAD_{ox}·$PchC_{red}$ complex (— — —), and the PchF[Y384F]$FADH_2$·$PchC_{red}$ complex (- - -). The inset shows the SPECFIT-calculated concentrations of each component as a function of *p*-cresol concentration. Similar results were obtained when 4-hydroxybenzyl alcohol was used as the titrant.

product, 4-hydroxybenzyl alcohol) so that the molar ratio of added *p*-cresol to reduced PCMH[Y384F] was 3:4. For an anaerobic 4-hydroxybenzyl alcohol titration, this ratio is 3:2. Unlike the titration of PCMH with *p*-cresol (*4*), the intermediate formation of a (anionic) flavin radical was not observed during the analogous titration of PCMH[Y384F].

Redox Potentials. The two-electron midpoint redox potentials, $E_{m,7}$ (NHE in 25 mM KH_2PO_4-KOH buffer (pH 7.0) at 25 °C), for various subunits and their combinations were measured according to the procedure of Massey (*5*) by using appropriate reference redox dyes, xanthine and xanthine oxidase as the electron source, and methyl viologen as the carrier of electrons from xanthine oxidase to other constituents. The veracity of the measured values of $E_{m,7}$ is re-enforced by the fact that nearly the same values were obtained for a particular protein when two or three reference dyes were used (Table 1).

In the absence of a reference dye, the complete reduction of $PchF^C$, PCMH, $PchF^{NC}$, PchF[Y384F]FAD, or PCMH-[Y384F] proceeded with the intermediate formation of the flavin anionic radical. In all cases, the rate of formation of the flavin radical was considerably faster than the rate of its subsequent reduction. The spectral data sets allowed for the determination of the values of $E_{m,7}$ (E_1 and E_2) for the following one-electron couples for $PchF^C$, $PchF^{NC}$, and PchF-[Y384F]FAD.

$$F_{ox} + e^- \rightleftharpoons F_{rad} \qquad E_1 \qquad \text{(I)}$$

$$F_{rad} + e^- \rightleftharpoons F_{red} \qquad E_2 \qquad \text{(II)}$$

The results of one such experiment are depicted in Figure 6. For reactions I and II, F_{ox}, F_{rad}, and F_{red} are the oxidized, the one-electron reduced, and the fully two-electron reduced forms of these flavoproteins, respectively. Equation 1 is valid if the system is at equilibrium (*19*):

$$\left(\frac{[F_{rad}]}{[F]_t}\right)_{max} = \frac{\sqrt{K}}{2+\sqrt{K}} \qquad (1)$$

where $[F]_t = [F_{ox}] + [F_{rad}] + [F_{red}]$ and K, the "semiquinone formation constant" (*19*), is defined as $[F_{rad}]^2/([F_{ox}][F_{red}])$. By definition

$$\Delta E = E_1 - E_2 = (RT/NF)\ln(K) \qquad (2)$$

where R is the gas constant, T is the temperature (298 K), N (=1) is the number of electrons per mole transferred in each phase, and F is Faraday's constant. With rapid equilibration among the various oxidation states of the bound FAD, Factor Analysis of the spectral set obtained from the reduction of the flavoproteins by the xanthine/xanthine oxidase/methyl viologen electron-generating system provided good estimated values of $([F_{rad}]/[F]_t)_{max}$ for $PchF^C$, $PchF^{NC}$, and PchF[Y384F]-FAD, which were 0.87, 0.71, and 0.64, respectively, and these parameters yielded K values of 179, 24.0, and 12.6 (eq 1), respectively. In turn, these were used to calculate ΔE values of 133, 81, and 65 mV (eq 2), respectively. Since $(E_1 + E_2)/2 = E'$, the two-electron $E_{m,7}$, then $E_1 = E' + \Delta E/2$ and $E_2 = E' - \Delta E/2$. For $PchF^C$, $E' = 62$ mV and, therefore, $E_1 = 129$ mV and $E_2 = -5$ mV. For $PchF^{NC}$, $E' = -15$ mV and, therefore, $E_1 = 26$ mV and $E_2 = -55$ mV. For PchF[Y384]FAD, $E' = 2$ mV and, therefore, $E' = 35$ mV and $E_2 = -31$ mV.

Table 1: Two-Electron Redox Potentials for the FAD, and One-Electron Redox Potentials for the Heme Bound to Various Forms of PCMH and Its Unassociated Subunits

protein[a]	measured $E_{m,7}$ (slope)[b] (mV)	reference dye[c]	reference dye $E_{m,7}$ (mV)
PchF[Y384F]FAD	2 (0.94)	gallocyanine	21
	1.2 (0.92)	gallocyanine	21
	3[d]	juglon	3
$PchF^{NC}$	−15.6 (0.93)	gallocyanine	21
	−13.3 (1.00)	gallocyanine	21
$PchF^{C}$	59.5 (1.07)	thionin[e]	60
	61 (0.95)	thionin	60
	60 (1.11)	toluidine blue	34
	65.5 (0.98)	toluidine blue	34
	66 (1.06)	toluylene blue	115
PchC[f]	157 (1.98)	toluylene blue	115
	157 (2.05)	DCIP	218
	187[g]		
PchF[Y384F]FAD·PchC ≡ PCMH[Y384F]{FAD}[h]	49 (1.06)	toluidine blue	34
	46 (1.05)	toluidine blue	34
	45.5 (1.07)	thionin	60
PchF[Y384F]FAD·PchC ≡ PCMH[Y384F]{heme}[i]	186 (2.02)	DCIP	218
$PchF^{C}$/PchC ≡ PCMH{FAD}[h]	87 (0.99)	toluylene blue	115
	81 (1.09)	toluylene blue	115
$PchF^{C}$/PchC ≡ PCMH{heme}[f]	234 (1.97)	DCIP	218
	249[g]		

[a] The potentials are those for the prosthetic groups in braces. [b] The values in parentheses are the slopes of the $\log(dye_{ox})/\log(dye_{red})$ vs $\log(X_{ox})/\log(X_{red})$ plots (*5*), where X is FAD or heme. [c] Two entries for the same reference dye indicate the results of experiments involving different concentrations of xanthine oxidase. [d] The value was determined by Factor Analysis of the spectra obtained during the experiment, and not by fitting the data to an equation. [e] For thionin, an $E_{m,7}$ of 60 mV was used as the reference potential, which is midway between the values of 56 and 64 mV given in the literature (*19*). [f] The ratios of reduced and oxidized forms of PchC were determined from the peak at 418 nm. Since the changes in the absorbance were large at this wavelength, even low levels of reduction could be measured. For this reason, shifts of −60 and 40 mV, with respect to the reference dye, could be measured with confidence. [g] Values from the literature (*20*), which were determined potentiometrically. [h] The $E_{m,7}$ values are those for FAD in the presence of reduced heme because the $E_{m,7}$ values for the heme are significantly higher than those for FAD. [i] The PchC concentration was 2.5-fold higher than that of PchF[Y384F]FAD. In the presence of PchF[Y384F]FAD, the maximal absorbance for DCIP shifts from 600 to 650 nm. When PchC is present in excess, the binding of DCIP to protein is absent. Since approximately 40% of the total PchC is complexed with PchF[Y384F]FAD, the exact equation for the potential as a function of the level of reduction of PchC is complex, and is of little use in estimating the $E_{m,7}$ of PchC bound to PchF[Y384F]FAD. The measured potential of 186 mV should be viewed as a rough approximation rather than as an exact value.

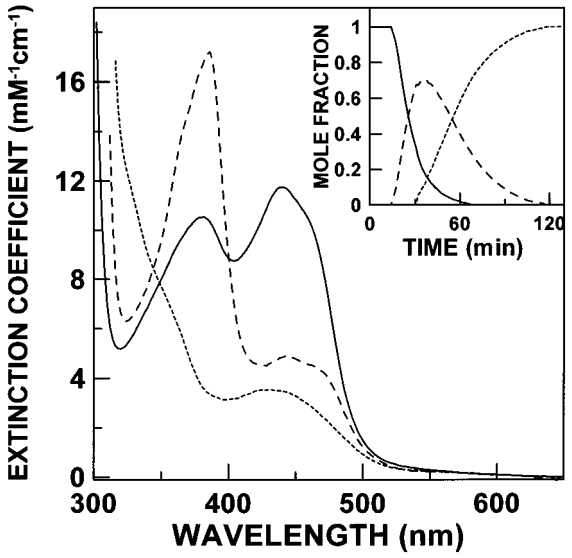

FIGURE 6: Results of the anaerobic reduction of $PchF^{NC}$ using xanthine and xanthine oxidase in the presence of methyl viologen. $PchF^{NC}$ was reduced in the presence of 300 μM xanthine, 50 nM xanthine oxidase, and 20 μM methyl viologen, in 25 mM KH_2PO_4-KOH buffer (pH 7.4) at 25 °C. The experiment was conducted over a period of 3 h, and spectra were recorded every 2 min. The results of the Factor Analysis of the spectral data are displayed in the figure, which shows the spectra of oxidized $PchF^{NC}$ (—), the FAD anionic "red" semiquinone radical (− − −), and the fully two-electron reduced flavin (- - -). The inset displays the mole fraction of each component as a function of time.

Similarly, the three one-electron potentials of PCMH and PCMH[Y384F] were estimated. Again, spectra were recorded for these proteins in an anaerobic solution with methyl viologen, xanthine, and catalytic levels of xanthine oxidase present, in the absence of a reference dye. The results of the experiment with PCMH are displayed in Figure 7. In this case, the formation constant for the first stage of the reduction of each flavocytochrome is defined as

$$K_1 = \frac{[F_{ox}C_{red}]^2}{[F_{ox}C_{ox}][F_{rad}C_{red}]} \quad (3)$$

and leads to the equation

$$\left(\frac{[F_{ox}C_{red}]}{[FC]_t}\right)_{max} = \frac{\sqrt{K_1}}{2+\sqrt{K_1}} \quad (4)$$

For this case, the following reactions apply:

$$F_{ox}C_{ox} + e^- = F_{ox}C_{red} \qquad E_a \qquad \text{(III)}$$

$$F_{ox}C_{red} + e^- = F_{rad}C_{red} \qquad E_b \qquad \text{(IV)}$$

$$F_{rad}C_{red} + e^- = F_{rad}C_{red} \qquad E_c \qquad \text{(V)}$$

For reactions III−V, F_{ox}, F_{rad}, and F_{red} are as defined above for reactions I and II and C_{ox} and C_{red} are the oxidized and one-electron-reduced forms of PchC, respectively. For PCMH and PCMH[Y384F], the values of $([F_{ox}C_{red}]/[FC]_t)_{max}$ were 0.90 and 0.78, respectively, which provided K_1 values of 324 and 50.3, respectively. Using eq 2, the values of ΔE_1 ($=E_a - E_b$) were found to be 149 and 101 mV, respectively.

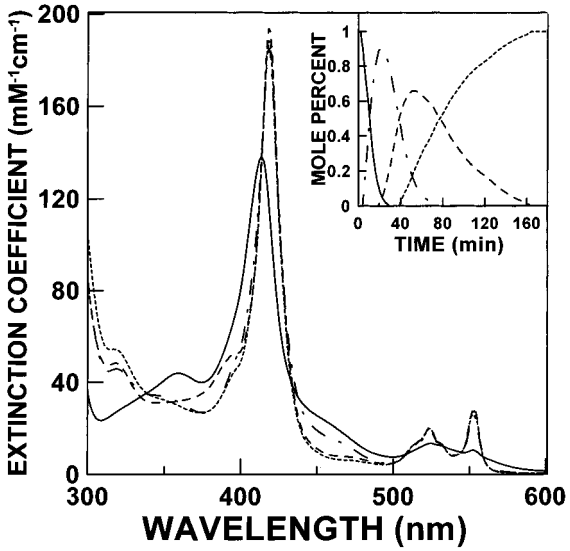

FIGURE 7: Results of the anaerobic reduction of PCMH using xanthine and xanthine oxidase in the presence of methyl viologen. PCMH was reduced in the presence of 300 μM xanthine, 50 nM xanthine oxidase, and 20 μM methyl viologen, in 25 mM KH_2PO_4-KOH buffer (pH 7.4) at 25 °C. The experiment was carried out over a period of 3 h, and spectra were recorded every 2 min. The results of the Factor Analysis of the spectral data are displayed in the figure, which shows the spectra of oxidized PCMH (—), the one-electron-reduced PCMH (− - −) (only the heme prosthetic group is reduced), the two-electron-reduced enzyme (− − −) (reduced heme and FAD anionic "red" radical), and the fully three-electron-reduced enzyme (- - -). The inset displays the mole fraction of each component as a function of time.

Following the same procedure, the values of K_2 (eq 5) can be determined.

$$K_2 = \frac{[F_{rad}C_{red}]^2}{[F_{ox}C_{red}][F_{red}C_{red}]} \quad (5)$$

The values of $([F_{rad}C_{red}]/[FC]_t)_{max}$ were 0.66 and 0.78 for PCMH and PCMH[Y384F], respectively, which provided K_2 values of 15.1 and 50.3, respectively, and from eq 2, ΔE_2 ($=E_b - E_c$) was found to be 70 and 101 mV, respectively. From the E_a value for PCMH (i.e., the $E_{m,7}$ for bound PchC, 234 mV from the current study and 249 mV from ref *20*; see Table 1) and from the ΔE_1 and ΔE_2 values, an E_b of 85 mV (=100 mV using the literature value of E_a) and an E_c of 15 mV (=30 mV, using an E_b of 100 mV) were calculated for wild-type PCMH (Table 2). Similarly, for PCMH-[Y384F], the values of E_a, E_b, and E_c were found to be 186 ($=E_{m,7}$ from Table 1), 87, and −14 mV, respectively (Table 2).

Stopped-Flow Studies of the Reduction of PchF[Y384F]-FAD and PchC$_{ox}$ by Substrates. All of the transient spectral changes for substrate reduction of $PchC_{ox}$ were biphasic. Depending on the $PchC_{ox}$ concentration, the first phase of reduction (40−80% of the reaction) occurred within 30−50 ms of mixing. This rapid, exponential transient was followed by a slower linear change. Complete PchC reduction was achieved after several minutes. The rate of the second phase was dependent on temperature and on the concentrations of PchF[Y384F]FAD, $PchC_{ox}$, and the substrate. Figure 8 shows a set of transients recorded at 552 nm for the 4-hydroxybenzyl alcohol reduction of $PchC_{ox}$ and PchF[Y384F]FAD. To account for the spectral changes, and to extract the values for the kinetic parameters for the process, a model was derived, which is based on the assumptions that PchF[Y384F]-FAD does not bind $PchC_{ox}$ stiochiometrically and unassociated $PchC_{ox}$ accepts electrons from PchF[Y384F]FAD_{rad}• $PchC_{red}$ (the two-electron-reduced substrate species containing reduced heme and the FAD radical).

The model allowed the determination of the K_D value for the PchF[Y384F]FAD−$PchC_{ox}$ interaction and of the values

Table 2: Estimated Values for One-Electron Redox Potentials for the FAD and the Heme Prosthetic Groups of Various Forms of PchF and PCMH[a]

species	E_a (mV)	E_b (mV)	E_c (mV)	$E_{m,7}$[b] (calcd $E_{m,7}$)[c] (mV)
$PchF^C$	NA[d]	129	−5	62
$PchF^{NC}$	NA[d]	26	−55	−15
PchF[Y384F]	NA[d]	35	−31	2
PCMH	234[e]	85	15	(50) 84
	249[f]	100	30	(65)
PCMH[Y384F]	186	87	−14	(37) 47
protein-free 8α-*O*-tyrosylriboflavin	NA[d]	ND[g]	ND[g]	−169[h]
protein-free riboflavin[i]	NA[d]	−231	−167	−199

[a] E_a, E_b, and E_c are the estimated one-electron potentials for, respectively, heme reduction, formation of the FAD anionic radical from the fully oxidized flavin, and reduction of the radical to the fully two-electron reduced form of bound FAD. [b] The values for the two-electron potential of the flavin, which are the averages of the values in Table 1. [c] The values in parentheses are the two-electron potentials calculated from the equation $E_{m,7} = (E_b + E_c)/2$. [d] Not applicable. [e] Determined in the study presented here. [f] From ref *20*. [g] Not determined. [h] Estimated from the K_D value for binding of sulfite to 8α-*O*-tyrosylriboflavin (*26*). [i] From ref *23*.

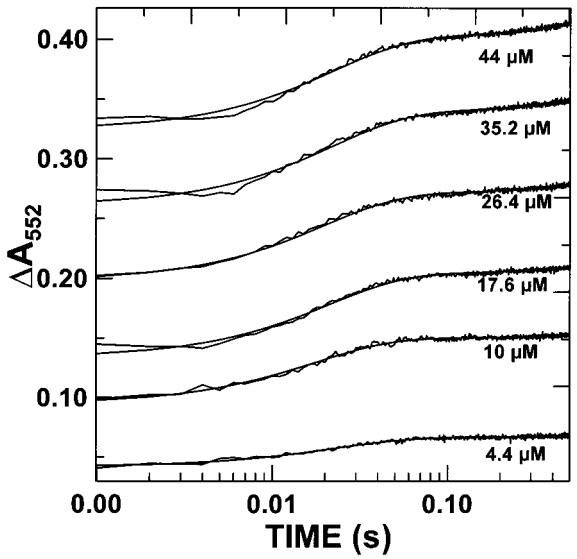

FIGURE 8: Rapid reaction of PCMH[Y384F] with 4-hydroxybenzyl alcohol. The stopped-flow reactions were carried out in 25 mM KH_2PO_4-KOH buffer (pH 7.4) at 6 °C. The change in the absorbance at 552 nm is shown as a function of time (the dead time was less than 2 ms). One syringe contained PchF[Y384F]-FAD and PchC, and the second syringe contained the substrate. For each reaction, the final concentration of PchF[Y384F]FAD was 4.8 μM (monomer concentration), and the total concentration of 4-hydroxbenzyl alcohol was 100 μM. The semilog plots of the data highlight the slow linear phase of the absorbance change at each PchC concentration. The PchC concentration for each reaction is provided in the figure. The smooth lines show the nonlinear fits of the traces to eq 8 (see the text).

of the rate constants for the two phases observed in the reduction of $PchC_{ox}$ after mixing of PchF[Y384F]FAD with $PchC_{ox}$ and substrate. In the following equations, PchF-[Y384F]FAD is designated as F, PchC as C_{ox} and C_{red} for the oxidized and reduced forms, respectively, and oxidized and one-electron-reduced PCMH[Y384F] are abbreviated as FC_{ox} and FC_{red}, respectively. 4-Hydroxybenzyl alcohol is abbreviated as *alc* and 4-hydroxybenzaldehyde as *ald*. The absorbance change at 552 nm is due to the reduction of C_{ox} and FC_{ox}. The first electron from the substrate, two-electron-reduced FAD, is transferred rapidly to the bound cytochrome:

$$alc + FC_{ox} \rightarrow ald\cdot F^{\bullet}C_{red} \qquad \text{(VI)}$$

$$-\frac{d[ald\cdot F^{\bullet}C_{red}]}{dt} = \frac{d[FC_{ox}]}{dt} = -k_1[FC_{ox}] \qquad (6)$$

where $F^{\bullet}$ is PchF[Y384F]FAD$^{\bullet}$ (the flavoprotein radical) and k_1, a function of [*alc*], is yet to be defined. The second reaction represents the transfer of an electron from $F^{\bullet}C_{red}$ to free C_{ox}:

$$ald\cdot F^{\bullet}C_{red} + C_{ox} \rightarrow ald\cdot FC_{red} + C_{red} \qquad \text{(VII)}$$

$$\frac{d[C_{ox}]}{dt} = -k_2[ald\cdot F^{\bullet}C_{red}] \qquad (7)$$

In eq 7, k_2 is a function of $[C_{ox}]$. The final expression simplifies because reaction VI is more than 10 times faster than reaction VII; i.e., when the first reaction is complete, the second reaction is still in its initial stage. Thus, eqs 6 and 7 can be integrated independently when $[ald\cdot F^{\bullet}C_{red}] = [FC_{ox}]$, the concentration of bound $PchC_{ox}$ at time zero. The analysis simplifies by recognizing that the ϵ_{552} of $PchC_{red}$ is the same whether it is bound to PchF[Y384F]FAD. The same is true for free and bound $PchC_{ox}$ (*1*). Therefore, the absorbances from both reactions can be added together to yield the following equation for stopped-flow kinetic traces at 552 nm:

$$A_{552}(t) = \epsilon_{ox}[C_{ox}] + (\epsilon_{red} - \epsilon_{ox})(1 - e^{-k_1 t})[FC_{ox}] + k_2 t(\epsilon_{red} - \epsilon_{ox})[FC_{ox}] \qquad (8)$$

where ϵ_{ox} (6.6 mM^{-1} cm^{-1}) and ϵ_{red} (25.6 mM^{-1} cm^{-1}) are the extinction coefficients for $PchC_{ox}$ and Pch_{red} at 552 nm, respectively, and $[C_{ox}]$ is the initial total concentration of $PchC_{ox}$. The transients in Figure 8 were fit to eq 8 by nonlinear regression analysis. At each concentration of C_{ox}, the values of $[FC_{ox}]$, k_1, and k_2 were obtained.

The values for $[FC_{ox}]$ generated by the nonlinear regression analysis are plotted in Figure 9 as a function of $[C_{ox}]$. The curve was fit to the following (quadratic) equation:

$$[FC_{ox}] = \frac{[F] + [C_{ox}] + K_D - \sqrt{([F] + [C_{ox}] + K_D)^2 - 4[F][C_{ox}]}}{2} \qquad (9)$$

and yielded a K_D of 2.8 ± 0.5 μM at 6 °C for the FC_{ox} complex. At 25 °C, the K_D value was found to be 7.4 ± 0.7 μM (data not shown).

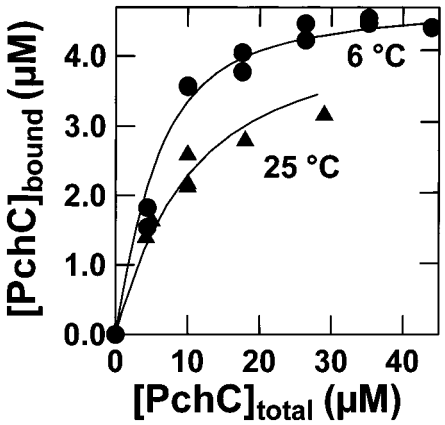

FIGURE 9: Effect of the total PchC concentration on the binding of PchF[Y384F]FAD to PchC. The concentrations of PCMH-[Y384F] (which equals $[FC_{ox}]$ which equals $[PchC]_{bound}$) at time zero were determined by nonlinear regression analyses of the stopped-flow traces shown in Figure 8 by using eq 8. A plot of the combined data (●) obtained for the reduction of PCMH[Y384F] by 4-hydroxybenzyl alcohol and *p*-cresol at 6 °C. The monomer concentration of PchF[Y384F]FAD was 4.8 μM. A plot of the data (▲) obtained from the 4-hydroxybenzyl alcohol reduction of PCMH-[Y384F] at 25 °C is shown also. The monomer concentration of PchF[Y384F]FAD was 4.5 μM. The nonlinear regression analyses of the plots for 6 and 25 °C (solid lines), using eq 9, provided K_D values of 2.8 ± 0.5 and 7.4 ± 0.7 μM, respectively. The standard error for each $[PchC]_{bound}$ value in these plots was approximately ±0.005, which is encompassed by the symbols.

Plots of k_2 versus $[PchC_{ox}]$ for the reactions at 6 and 25 °C (data not shown) provided values for the slopes, k_2/K_{D2} ($\equiv k_{cyt}$), of 7200 ± 280 M^{-1} s^{-1} at 6 °C and 10 700 ± 1800 M^{-1} s^{-1} at 25 °C, respectively, where K_{D2} is the dissociation constant for the interaction of C_{ox} with $ald\cdot F^{\bullet}C_{red}$ (reaction VII). The linearity of the plots indicated that the value of K_{D2} for $PchC_{ox}$ as the electron acceptor for PchF[Y384F]-FAD·$PchC_{red}$ is far larger than the concentrations of $PchC_{ox}$ used in the study.

It was found that the k_1 values were independent of $[PchC_{ox}]$ (data not shown); the mean value of k_1 was 46.5 ± 0.4 s^{-1}. This justified the assignment of the rapid process as a reduction of PCMH[Y384F] by 4-hydroxybenzyl alcohol, which is in large excess. In separate experiments, k_1 was measured as a function of [*alc*] (5−150 μM at 6 °C), at constant equimolar concentrations (5 μM) of PchF[Y384F]-FAD and $PchC_{ox}$. The curve (Figure 10) was fit to eq 10:

$$k_1 = \frac{k_c[alc]}{K + [alc]} \qquad (10)$$

This equation was derived from the following reaction, assuming $k_d = 0$ (*21*):

$$alc + FC_{ox} \underset{k_b}{\overset{k_a}{\rightleftharpoons}} alc\cdot FC_{ox} \underset{k_d}{\overset{k_c}{\rightleftharpoons}} ald\cdot F^{\bullet}C_{red}$$

In eq 10, $K = (k_b + k_c)/k_a$ and is equal to K_D for the alcohol when $k_b > k_c$. Nonlinear regression analysis provided a K of 160 ± 18 μM and a k_c of 112 ± 8 s^{-1} [k_c/K = (7.05 ± 0.65) × 10^5 M^{-1} s^{-1}]. When the entire set of transients (Figure 8) was fit to eq 8, it was found, as expected (vide infra), that k_2 was independent of [*alc*].

For the experiment carried out at 25 °C (Figure 10), saturating concentrations of the alcohol could not be attained.

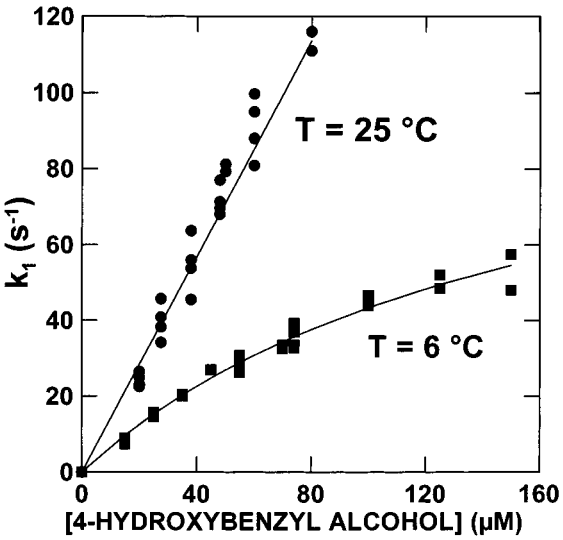

FIGURE 10: Effect the of 4-hydroxybenzyl alcohol concentration on the rate constant, k_1, for the reduction of FC_{ox}. The k_1 values were determined by nonlinear regression analyses of the stopped-flow traces (data not shown) by using eq 8. The experiments were carried out in 25 mM KH_2PO_4-KOH buffer (pH 7.4) at 6 and 25 °C. The equimolar monomer concentrations of PchF[Y384F]FAD and PchC were maintained at 5 μM. The solid lines show the nonlinear regression fit of the data obtained at 6 °C to eq 10 (see the text), and the linear regression fit to the data obtained at 25 °C. The errors in k_1 are approximately 3 and 0.6% of the k_1 values for the data obtained at 25 and 6 °C, respectively.

The effective bimolecular rate constant, k_c/K, was $(1.42 \pm 0.03) \times 10^6$ M^{-1} s^{-1}. The reduction was much slower using *p*-cresol as the substrate at 25 °C (the plot of k_1 vs [*p*-cresol] was hyperbolic; data not shown); $k_c = 18.7 \pm 0.84$ s^{-1}, and $K = 16 \pm 2$ μM [$k_c/K = (1.17 \pm 0.22) \times 10^6$ M^{-1} s^{-1}]. For wild-type PCMH, these values were as follows: $k_c = 185 \pm 3.0$ s^{-1} and $K = 16 \pm 3$ μM [$k_c/K = (11.6 \pm 0.8) \times 10^6$ M^{-1} s^{-1}] (*14*). When the experiment was repeated using 4-[$^2H_3$]methylphenol (i.e., α-trideuterated *p*-cresol), it was found that the ^Dk_c isotope effect was 7, the same value found for the intrinsic deuterium isotope effect for the reaction of wild-type PCMH with *p*-cresol and 4-[$^2H_3$]methylphenol (*14*, *22*).

Equations 8−10 were combined into one formula that is valid for the reduction of PchF[Y384F]FAD and $PchC_{ox}$ by *p*-cresol or 4-hydroxybenzyl alcohol (designated as S):

$$A_{552}(t) = \epsilon_{ox}[C_{ox}] + (\epsilon_{red} - \epsilon_{ox})[1 - e^{-k_c t[S]/(K+[S])}] [FC_{ox}] + k_{cyt} t(\epsilon_{red} - \epsilon_{ox})[FC_{ox}][C]_t \quad (11)$$

where $[FC_{ox}]$ is obtained from eq 9. Note that $[C]_t$ in eq 11 is the total [PchC] and not the concentration of free PchC, as required by eq 7, since after reaction VII, the electron in *ald*·FC_{red} may be transferred also to a bound $PchC_{ox}$:

$$ald\cdot FC_{red} + FC_{ox} \rightarrow ald\cdot FC_{ox} + FC_{red} \quad \text{(VIIa)}$$

A correct treatment in this case is complicated and does not lead to eq 11. Introduction of $[C]_t - [FC]$ instead of $[C]_t$ in eq 11 does not allow for the solution of the pertinent parameters. Fortunately, due to the rapidity of reaction VI, the contribution of reaction VIIa is insignificant.

In addition to reactions VI and VII, another reaction may occur whereby electrons are transferred directly from PchF-[Y384F]FAD to free $PchC_{ox}$, since it is known that alcohol reduces FAD bound to PchF[Y384F]:

$$alc\cdot F + 2C_{ox} \rightarrow ald\cdot F + 2C_{red} \quad \text{(VIII)}$$

In this case, the third term in eq 11 would contain $([F] - [FC])[C_{ox}]$. Nonlinear regression fitting of the data to this formula did not produce a value for the constant k_{cyt}. For this reason, reaction VIII was ignored. Table 3 lists the best-fit constants to eq 11, for both substrates.

DISCUSSION

Stability of the PchF[Y384F]FAD·PchC$_{red}$ Complex. The interaction of PchF[Y384F] with PchC may be represented by the following thermodynamic cycle:

$$\begin{array}{ccc} \text{PchF[Y384F]FAD•PchC}_{ox} & \overset{E_x}{\rightleftharpoons} & \text{PchF[Y384F]FAD•PchC}_{red} \\ \Downarrow K_x & & \Downarrow K_y \\ \text{PchF[Y384F]FAD + PchC}_{ox} & \overset{E_y}{\rightleftharpoons} & \text{PchF[Y384F]FAD + PchC}_{red} \end{array}$$

where E_x and E_y are the one-electron potentials of PchC bound to the flavoprotein subunit and free PchC, respectively, and K_x and K_y are dissociation constants. Thus, it follows that

$$\frac{RT}{F}\ln\left(\frac{K_x}{K_y}\right) = E_x - E_y \quad (12)$$

It was found that the $E_{m,7}$ values of bound PchC were more positive than those of the unassociated forms. This shift was most pronounced for wild-type PCMH (80 mV). For PchF-[Y384F]FAD, a 30 mV shift was measured for PCMH-[Y384F]. From eq 12, it follows that $K_x > K_y$, indicating that reduced PchC binds more tightly than its oxidized form. This difference is hardly manifested for wild-type PCMH, since the subunit K_D value is very small (6 nM for $PchF^C$ and $PchC_{ox}$) (*1*), whereas the subunit K_D value for PCMH-[Y384F] is ∼7 μM. The different affinities allow hydroxyapatite chromatography to separate the subunits for PCMH-[Y384F] but not for PCMH. The relative positive shift in the $E_{m,7}$ could also account for the observation that the reoxidation of bound PchC by oxygen is slow for the PchF-[Y384F]FAD·$PchC_{red}$ complex.

Reductive Titration of the Flavoprotein Subunit by Substrates. Reduction of the flavin occurs when the two-electron $E_{m,7}$ of the substrate is more negative than that of the cofactor. Otherwise, the substrate will bind and, perhaps, form a weak charge transfer complex with FAD, and may reduce the flavin very slowly, as was observed in the case of the interactions of $PchF^{NC}$ (*2*) and PchF[Y384F]FAD with *p*-cresol. From our past (*2*) and present work, the following scale of two-electron redox potentials can be proposed:

$$E_{PchF^C} \gg E_{PchF[Y384F]FAD} > E_{p-cresol} > E_{PchF^{NC}} \gg E_{alcohol}$$

The two-electron $E_{m,7}$ of the active site *p*-cresol/4-hydroxybenzyl alcohol couple was estimated to be about −5 to −10 mV (see Table 1). The $E_{m,7}$ for the 4-hydroxybenzyl alcohol/4-hydroxybenzaldehyde couple is far more negative. Unpublished experiments have shown that apo-PchF reconstituted with 5-deaza-FAD was reduced by the alcohol at a

Table 3: Kinetic and Equilibrium Parameters for PCMH[Y384F]

substrate [T (°C)]	apparent K_D (μM)	k_c (s^{-1})	k_c/K_D ($\times 10^{-5}$ M^{-1} s^{-1})	K_D (μM)[a]	k_{cyt} ($\times 10^{-3}$ M^{-1} s^{-1})
p-cresol (25)	16 ± 2	18.7 ± 0.8	11.7 ± 2.2	7.4 ± 0.7	12 ± 1
alcohol[b] (25)	ND[c]	ND[c]	14.2 ± 0.3	7.4 ± 0.7	12 ± 1
alcohol[b] (6)	160 ± 18	112 ± 8	7.05 ± 0.65	2.8 ± 0.5	6.8 ± 1.5

[a] The K_D values for interaction of PchF[Y384F] with PchC. [b] Alcohol is 4-hydroxybenzyl alcohol. [c] Not determined.

reasonable rate, indicating that the two-electron $E_{m,7}$ of the alcohol/aldehyde couple is lower than that of the two-electron $E_{m,7}$ of bound 5-deaza-FAD, which is expected to be considerably lower than that for bound FAD; the $E_{m,7}$ values for free riboflavin and 5-deazariboflavin are −199 and approximately −290 mV, respectively (*23*). Significantly, our findings with the 5-deaza-FAD-reconstituted enzyme indicate that the oxidation of the substrate by PCMH occurs via a hydride transfer from the substrate to the N(5) position of the flavin isoalloxazine ring, since 5-deaza-FAD is a mandatory two-electron acceptor (*24*).

Setting the above $E_{m,7}$ scale presumed that the rates of the reactions of *p*-cresol and 4-hydroxybenzyl alcohol with the various forms of PchF were determined solely by thermodynamic considerations (i.e., differences in $E_{m,7}$ values). However, there may be a kinetic barrier preventing facile *p*-cresol reduction of PchF[Y384F]FAD and $PchF^{NC}$, in contrast to the rapid 4-hydroxylbenzyl alcohol reduction. Some of the data in Table 3 suggest that the alcohol is a "better" substrate for PCMH[Y384F] than *p*-cresol (the k_c/K value for the alcohol is greater than that for *p*-cresol at 25 °C). On the other hand, steady-state kinetic analyses with PCMH indicated that *p*-cresol was the better substrate (*4*). Thus, it is prudent to remain cautious with regard to predicting the relative rates of reactions solely on the basis of thermodynamic driving forces. There may be structural alterations at the active sites and/or at the FAD binding sites within $PchF^{NC}$, $PchF^{C}$, PCMH, PchF[Y384F]FAD, and PCMH[Y384F] that, at least in part, might account for the different reactivities toward *p*-cresol and 4-hydroxybenzyl alcohol.

One- and Two-Electron Redox Potentials. There is a dramatic increase in its two-electron $E_{m,7}$ when FAD binds to apo-PchF or apo-PchF[Y384F] (∼185 and ∼200 mV, respectively) (Table 1). Obviously, there must be significant interactions with the proteinaceous environment to produce such dramatic shifts. Note that the two-electron $E_{m,7}$ of PchF-[Y384F]FAD is somewhat more positive than that for $PchF^{NC}$ (Table 1). This may be due to an unfavorable interaction between the negative charge of an unprotonated Tyr384 phenolate oxygen and the anionic fully reduced FAD ($FADH^-$) of $PchF^{NC}$. The phenolic proton of Tyr384 must be removed by a base on the enzyme (see B_X of structure **A** in Figure 1) for the covalent bond to form between Tyr384 and FAD in wild-type PchF (step 2 in Figure 1), following the binding of PchC to $PchF^{NC}$ (*2*, *9*, *25*). However, the differences in the $E_{m,7}$ for PchF[Y384F]FAD and $PchF^{NC}$ may be due to a change in the stereochemistry of the FAD binding site. The extra OH group on Tyr384 of $PchF^{NC}$ may sterically alter the manner in which FAD binds relative to the way in which it binds in PchF[Y384F]FAD where this group is absent.

The two-electron $E_{m,7}$ for FAD covalently bound to PchC-free PchF is ∼75−80 mV more positive than for FAD noncovalently bound to this subunit (Table 1), and is 45−50 mV more positive than that predicted from the $E_{m,7}$ values for free riboflavin and 8α-*O*-tryosylriboflavin (Table 2). From this observation, we conclude that covalent flavinylation induces a change in the environment of the isoalloxazine ring via a conformational change. The $E_{m,7}$ for the covalently bound FAD increases by ∼20 mV when PchC binds to $PchF^{C}$, which indicates that the environment of the flavin ring has been altered again, perhaps through a conformational change or altered electrostatic interactions with PchC.

To measure the two-electron $E_{m,7}$ values, xanthine, xanthine oxidase (the electron generator), methyl viologen (the electron mediator), and a redox reference dye with a known $E_{m,7}$ were used. Full reduction of the FAD bound to PchF-[Y384F], $PchF^{C}$, $PchF^{NC}$, PCMH, or PCMH[Y384F] occurred without the intermediate formation of the anionic FAD radical. This was curious because, during the course of the dithionite titrations of $PchF^{C}$ (*2*) and PCMH (*4*, *26*), nearly stoichiometric formation of the FAD radical occurred. For PchF[Y384F], PCMH[Y384F], or $PchF^{NC}$ (*2*), very little or no radical was produced in the course of the dithionite titrations. It was concluded that the reference dyes were two-electron-reduced by the methyl viologen radical because, presumably, the radical forms of these dyes are very unstable. Thus, the reduction or reoxidation of protein-bound FAD via a reference dye was a mandatory two-electron process. Since dithionite can act as a one- or two-electron donor, and depending on the redox (and other unrecognized) properties of the bound FAD and the various proteins, the formation of a significant amount of protein-bound flavin radical may or may not be seen when an electron transfer mediator is absent. For example, more than 90% of the anionic flavin radical formed during the dithionite titration of $PchF^{C}$, whereas at most, only a few percent of this radical formed during the dithionite titration of $PchC^{NC}$. Note that the value of the $E_{m,7}$ for the conversion of oxidized bound FAD to the radical for $PchF^{C}$ is 129 mV (Table 2), which is about 100 mV more positive than the corresponding one-electron $E_{m,7}$ for $PchF^{NC}$, and more than 130 mV more positive than the one-electron $E_{m,7}$ for the reduction of the radical to the fully reduced flavin in $PchF^{C}$ (Table 2). Thus, for $PchF^{C}$, there is a larger thermodynamic driving force for the one-electron reduction of fully oxidized FAD to the radical than there is for the same process with $PchF^{NC}$, or for the one-electron reduction of the radical to the two-electron-reduced flavin in $PchF^{C}$.

Depending on the protein, it was possible to generate from 64 to 90% of the total flavin as the flavin radical for $PchF^{C}$, $PchF^{NC}$, PchF[Y384F]FAD, PCMH[Y384F], and PCMH by using xanthine and xanthine oxidase to generate electrons in the presence of methyl viologen, in the absence of a reference dye. Following the lead of others (*5*, *7*), the system was assumed to be always at equilibrium, since very high

levels of methyl viologen were present during all the experiments. By applying Factor Analysis to the obtained spectra, we accurately determined the maximum amount of radical that formed. As a result, values for the two one-electron redox potentials of the bound FAD (Table 2) were calculated by using the one-electron $E_{m,7}$ for the heme and the two-electron $E_{m,7}$ values for the bound FAD (Table 1).

Reactions of Substrates with PCMH. The binding of PchC to $PchF^{C}$ and Pch[Y384F]FAD shifts dramatically upward the two-electron $E_{m,7}$ of the flavin (Table 1). Thus, the driving forces for the oxidation of the substrates increase, as do the rate constants for reduction. Also note that the $E_{m,7}$ of FAD bound to PCMH is 30−40 mV greater than that for PCMH-[Y384F]. Again, the rate constant for the reduction of PCMH by *p*-cresol (185 s^{-1}) (*14*) is much greater than that for PCMH[Y384F] (18.3 s^{-1}) (Table 3), while the K_D values for the interaction of *p*-cresol with both forms of the flavocytochrome are similar (∼16 μM).

Covalent Flavinylation. Previously, we speculated that the covalent flavinylation of $PchF^{NC}$ occurred because of structural changes induced by the binding of PchC (*2*, *9*, *25*). The results presented here suggest that the binding of PchC to $PchF^{NC}$ causes a large increase in the $E_{m,7}$ of bound FAD, thereby making it a better electrophile for attack at its 8α-carbon by Tyr384 O^-. In effect, the increased $E_{m,7}$ makes the 8α-hydrogens more acidic (structure **B** in Figure 1), thereby allowing for a more efficient removal of one of these by a nearby base, and increasing the equilibrium concentration of the iminoquinone methide intermediate (Figure 1) required for nucleophilic attack. This potential shift was ∼45 mV [$E_{m,7}$(PCMH[Y384F]) − $E_{m,7}$(PchF[Y384F]FAD)]. This assumes that, other than the missing OH group of Tyr384, the structures of $PchF^{NC}$•PchC and PCMH[Y384F] are similar, and also that the structures of $PchF^{NC}$ and PchF-[Y384F]FAD are similar. It is interesting to note that the binding of PchC to $PchF^{C}$ increases the $E_{m,7}$ of the flavin by ∼25 mV, which is about 20 mV lower than the potential change that occurs when PchC binds to PchF[Y384F]FAD. All in all, on the basis of this new electrochemical information, it would appear that a combination of conformational changes (e.g., the proximity of the nucleophilic and electrophilic centers, and their relative orientations) coupled with an increase in the electrophilicity of the flavin contributes to efficient covalent flavinylation.

In addition to the 45 mV change in the $E_{m,7}$ of the FAD induced by the binding of PchC to $PchF^{NC}$, the covalent tethering of FAD seems to increase further the $E_{m,7}$ by ∼32−41 mV [$E_{m,7}$(PCMH) − $E_{m,7}$(PCMH[Y384F])]. For $PchF^{C}$ and $PchF^{NC}$, this increase is even greater; $E_{m,7}$($PchF^{C}$) − $E_{m,7}$-($PchF^{NC}$) ≈ 73−81 mV. A significant increase in $E_{m,7}$ following covalent bond formation is not unprecedented. The positive shift in the two-electron $E_{m,7}$ for VAO (the FAD is covalently bound to His422) relative to that of its H422A mutant (the FAD is noncovalently bound) is 110 mV (*7*). This is about the same as the total change in the flavin $E_{m,7}$ that occurs during formation of PCMH from its constituent parts, i.e., $PchF^{NC}$ → $PchF^{C}$ ($\Delta E_{m,7} \approx 80$ mV), $PchF^{C}$ + PchC → PCMH ($\Delta E_{m,7} \approx 25$ mV), or $PchF^{NC}$ + PchC → PCMH ($\Delta E_{m,7} \approx 105$ mV).

A very positive $E_{m,7}$ for an enzyme-bound flavin is unusual, but not unprecedented; for example, the two-electron $E_{m,7} = 55$ mV for FAD of VAO (*7*). The $E_{m,7}$ values for the flavins in other covalent flavoproteins have been measured, and in general are greater than the $E_{m,7}$ values in proteins containing noncovalently bound flavin: 28 mV (FAD/$FADH_2$) for the flavocytochrome from *Chlorobium thiosulfatophilum* (*27*), 44 mV (FMN/$FMN^{\bullet-}$) and 36 mV ($FMN^{\bullet-}$/$FMNH_2$) for the trimethylamine dehydrogenase from *Methylophilus methylotrophus* W3A1 (*28*), −74 mV (FAD/$FAD^{\bullet-}$) and −127 mV ($FAD^{\bullet-}$/$FADH_2$) for the cholesterol oxidase from *Brevibacterium sterolicum* (*29*), −55 mV (FAD/$FADH_2$) for the *E. coli* fumarate reductase (*30*), −60 to −90 mV (FAD/$FADH_2$) for the beef liver succinate dehydrogenase (*31*), and 80 mV (FAD/$FAD^{\bullet-}$) and 30 mV ($FAD^{\bullet-}$/$FADH_2$) for the bacterial thiamine dehydrogenase (*32*). To our knowledge, the two-electron $E_{m,7}$ for FAD in wild-type PCMH (81−87 mV) is the highest documented for an FAD- or FMN-containing protein.

Further Comparisons of VAO and PCMH. VAO and PCMH catalyze similar reactions (*33*), and their flavoprotein subunits have very similar three-dimensional structures (*6*). It has been shown that the three-dimensional structure of the flavoprotein subunit of the H422A mutant of VAO is virtually identical to that of wild-type VAO (*7*, *8*). In analogy, it is predicted that the structure of PchF[Y384F]FAD will also be similar to its wild-type counterpart.

Although the wild-type and mutant protein structures may be similar, the lack of covalent FAD attachment in the mutant proteins has a dramatic effect on their redox and kinetic properties. For example, while the K_M values for the reducing substrates for the VAO[H422A]FAD and PCMH[Y384F]-FAD mutant proteins are about the same as those determined for their wild-type counterparts (*7*), the k_{cat} values for the mutants are about an order of magnitude lower than those exhibited by the wild-type proteins.

The $E_{m,7}$ measurements for the FAD bound to the H422A mutant of VAO indicated that there was an intermediate formation of a neutral flavin radical (*7*). The method used to determine the potentials of VAO was identical to that used to measure the $E_{m,7}$ values in the study presented here (*5*). The values of the two one-electron redox potentials for VAO-[H422A] are −17 mV (FAD/$FADH^{\bullet}$) and −113 mV ($FADH^{\bullet}$/$FADH_2$) (*7*). The radical was not detected when wild-type VAO (*7*) or wild-type PCMH was reduced by the xanthine/xanthine oxidase/methyl viologen system, in the presence of a reference dye. However, during anaerobic dithionite titrations of wild-type VAO, PCMH, or $PchF^{C}$, a significant concentration of the anionic flavin radical formed as an intermediate (*2*, *26*, *34*).

The Raison d'Ĕtre for Covalent Flavin Tethering in PCMH. Previously, we concluded that the covalent bond between FAD and the polypeptide backbone of PchF in wild-type PCMH provided for a more efficient electron transfer pathway from substrate-reduced FAD to the oxidized heme of PchC (*6*, *9*). The evidence provided in the current report indicates that, in addition to this role, the covalent binding of FAD increases its two-electron $E_{m,7}$ dramatically, making it a better catalyst for the oxidation of *p*-cresol. Furthermore, the covalent binding of FAD to PchF provides for the tightest binding between the $PchF^{C}$ and PchC subunits.

The absence of the covalent bond in PCMH[Y384F] does not prevent electron transfer from substrate-reduced FAD to the heme, although the rate constant for heme reduction in PCMH[Y384F] is an order of magnitude lower than that

for PCMH. In past experiments, we showed that electron transfer from substrate-reduced FAD to heme in PCMH was much faster than the preceding reduction of FAD by the substrate (*14*, *22*). This is true also for PCMH[Y384F] because the reactions of *p*-cresol and 4-[$^2H_3$]methylphenol provided an intrinsic deuterium isotope effect of 7 for reduction of the heme in the wild-type (*6*, *9*) and mutant enzymes. Thus, even though the electron transfer path from FAD to heme has been disrupted following the removal of the *8*α-O-Tyr384 linkage in PCMH[Y384F], FAD reduction by *p*-cresol must be slower than electron transfer from fully reduced FAD to the oxidized heme.

In VAO, the covalent binding of FAD produces a large increase in the two-electron $E_{m,7}$ value (*7*). However, because it is an oxidase, electrons are transferred from the two-electron-reduced FAD directly to O_2 (*35*). Thus, the covalent FAD tethering in VAO is not required for electron transfer to another redox prosthetic group. In fact, the rate constant of oxidation of reduced FAD by O_2 is larger for the H422A mutant (2.5×10^5 M^{-1} s^{-1}) than for the wild-type oxidase (1.5×10^5 M^{-1} s^{-1}) (*7*). Additionally, the covalent attachment does not stabilize the oligomeric structure of VAO (*7*).

Finally, the covalent bond does not seem to be required for sequestering FAD from its environment. We have assessed tight noncovalent binding of 5-deaza-FAD (unpublished data) and FAD to apo-PchF (*2*), and tight binding of FAD to PchF[Y384F]. Additionally, FAD binds very tightly, but noncovalently, to the H422A, H422T, and H422C mutants of VAO (*7*).

Closing Remarks. From the current studies, it is concluded that the oxidative power of the FAD increases after it becomes covalently bound to PchF. This phenomenon likely results from a perturbation of the electronic properties of the flavin's isoalloxazine ring system caused directly by the covalent linkage, and from alterations in the proteinaceous environment of this ring system that occur upon formation of the covalent FAD bond. In addition, it is likely that further conformational changes, induced by the binding of PchC to $PchF^C$ or PchF[Y384F], increase further the oxidative power of the heme and flavin prosthetic groups. In collaboration with Scott Mathews' group (Washington University School of Medicine, St. Louis, MO), the 2.5 Å structure of PCMH has been determined (*6*) and its 1.8 Å structure is currently being refined. Dr. Mathews expects to determine the high-resolution structures of $PchF^C$, $PchF^{NC}$, apo-PchF[Y384F], and PchF[Y384F]FAD soon. The three-dimensional X-ray crystal structures of the pertinent proteins will provide valuable insights regarding the assertions stated above.

REFERENCES

1. Koerber, S. C., McIntire, W. S., Bohmont, C., and Singer, T. P. (1985) *Biochemistry 24*, 5276−5280.
2. Engst, S., Kuusk, V., Efimov, I., Cronin, C. N., and McIntire, W. S. (1999) *Biochemistry 38*, 16620−16628.
3. Cronin, C. N., and McIntire, W. S. (2000) *Protein Expression Purif. 19*, 74−83.
4. McIntire, W. S., Hopper, D. J., and Singer, T. P. (1985) *Biochem. J. 228*, 325−335.
5. Massey, V. (1991) in *Flavins and Flavoproteins* (Curti, B., Ronchi, S., and Zanetti, G., Eds.) pp 59−66, Walter de Gruyter & Co. New York.
6. Cunane, L. M., Chen, Z. W., Shamala, N., Mathews, F. S., Cronin, C. N., and McIntire, W. S. (2000) *J. Mol. Biol. 295*, 357−374.
7. Fraaije, M. W., van den Heuvel, R. H., van Berkel, W. J., and Mattevi, A. (1999) *J. Biol. Chem. 274*, 35514−35520.
8. Mattevi, A., Fraaije, M. W., Mozzarelli, A., Olivi, L., Coda, A., and van Berkel, W. J. (1997) *Structure 5*, 907−920.
9. Kim, J., Fuller, J. H., Kuusk, V., Cunane, L., Chen, Z.-W., Mathews, F. S., and McIntire, W. S. (1995) *J. Biol. Chem. 270*, 31202−31209.
10. Koerber, S. C., Hopper, D. J., McIntire, W. S., and Singer, T. P. (1985) *Biochem. J. 231*, 383−387.
11. Deng, W. P., and Nickoloff, J. A. (1992) *Anal. Biochem. 200*, 81−88.
12. Cronin, C. N. (1997) *Eur. J. Biochem. 247*, 1029−1037.
13. Cronin, C. N., Kim, J.-H., Fuller, J., Zhang, X.-P., and McIntire, W. S. (1999) *DNA Sequence 10*, 7−17.
14. McIntire, W. S., Hopper, D. J., and Singer, T. P. (1987) *Biochemistry 26*, 4107−4117.
15. Edmondson, D. E., and Singer, T. P. (1973) *J. Biol. Chem. 248*, 8144−8149.
16. Massey, V., and Hemmerich, P. (1978) *Biochemistry 17*, 9−16.
17. McIntire, W. S. (1983) Ph.D. Thesis, University of California, Berkeley, CA.
18. Pace, C. N., Vajdos, F., Fee, L., Grimsley, G., and Gray, T. (1995) *Protein Sci. 4*, 2411−2423.
19. Clark, W. M. (1972) *Oxidation−Reduction Potentials of Organic Systems*, Chapter 7, pp 184−203, Robert E. Kreiger Publishing Co., Huntington, NY.
20. Hopper, D. J. (1983) *FEBS Lett. 161*, 100−102.
21. Strickland, S., Palmer, G., and Massey, V. (1975) *J. Biol. Chem. 250*, 4048−4052.
22. McIntire, W. S., Everhart, E. T., Craig, J. C., and Kuusk, V. (1999) *J. Am. Chem. Soc. 121*, 5865−5880.
23. Stankovich, M. T. (1991) in *Flavins and Flavoproteins* (Müller, F., Ed.) Vol. I, pp 401−425, CRC Press, Boca Raton, FL.
24. Massey, V., and Hemmerich, P. (1980) *Biochem. Soc. Trans. 8*, 246−257.
25. Mewies, M., McIntire, W. S., and Scrutton, N. S. (1998) *Protein Sci. 7*, 7−20.
26. McIntire, W. S., Edmondson, D. E., Hopper, D. J., and Singer, T. P. (1981) *Biochemistry 20*, 3068−3075.
27. Meyer, T. E., Bartsch, R. G., Caffrey, M. S., and Cusanovich, M. A. (1991) *Arch. Biochem. Biophys. 287*, 128−134.
28. Barber, M. J., Pollock, V., and Spence, J. T. (1988) *Biochem. J. 256*, 657−659.
29. Gadda, G., Wels, G., Pollegioni, L., Zucchelli, S., Ambrosius, D., Pilone, M. S., and Ghisla, S. (1997) *Eur. J. Biochem. 250*, 369−376.
30. Ackrell, B. A. C., Cochran, B., and Cecchini, G. (1989) *Arch. Biochem. Biophys. 268*, 26−34.
31. Ackrell, B. A. C., Kearney, E. B., and Edmondson, D. E. (1975) *J. Biol. Chem. 250*, 7114−7119.
32. Gomez-Moreno, C., Choy, M., and Edmondson, D. E. (1979) *J. Biol. Chem. 254*, 7630−7635.
33. van den Heuvel, R. H., Fraaije, M. W., Laane, C., and van Berkel, W. J. (1998) *J. Bacteriol. 180*, 5646−5651.
34. de Jong, E., van Berkel, W. J. H., van der Zwan, R. P., and de Bont, J. A. (1992) *Eur. J. Biochem. 208*, 651−657.
35. Massey, V. (1994) *J. Biol. Chem. 269*, 22459−22462.

BI001644M